

## Phase Diagrams and Charge-Spin Separation in Two and Four Site Hubbard Clusters

Armen N. Kocharian

*Department of Physics and Astronomy,  
California State University, Northridge,  
CA 91330-8268*

Gayanath W. Fernando

*Department of Physics, University of Connecticut,  
Storrs, CT 06269 and IFS, Hantana Rd., Kandy, Sri Lanka*

James W. Davenport

*Computational Science Center,  
Brookhaven National Laboratory,  
Upton, NY 11973*

Charge spin separation, pseudogap formation and phase diagrams are studied in two and four site Hubbard clusters using analytical diagonalization and grand canonical ensemble method in a multidimensional parameter space of temperature, magnetic field, on-site Coulomb interaction ( $U \geq 0$ ), and chemical potential. The numerically evaluated, exact expressions for charge and spin susceptibilities provide clear evidence for the existence of true gaps in the ground state and pseudogaps in a limited range of temperature. In particular, Mott-Hubbard type charge crossover, spin pseudogap and magnetic correlations with antiferromagnetic (spin) pseudogap structure for two and four site clusters closely resemble the pseudogap phenomena and the normal-state phase diagram in high  $T_c$  superconductors.

PACS numbers: 65.80.+n, 73.22.-f, 71.27.+a, 71.30.+h

Understanding the effects of electron correlations and pseudogap phenomena [1, 2, 3, 4, 5, 6] in the cuprate superconductors comprising of many different phases is regarded as one of the most challenging problems in condensed matter [7]. Although the experimental determination of various inhomogeneous phases in cuprates is still somewhat controversial [8], the underdoped high  $T_c$  superconductors are often characterized by crossover temperatures below which excitation pseudogaps in the normal-state are seen to develop [9]. There is also compelling evidence for the existence of quantum critical points (QCPs) in underdoped [10, 11, 12] and optimally doped materials [13] as observed in resistivity measurements in  $\text{Nd}_{2-x}\text{Ce}_x\text{CuO}_{4\pm\delta}$ ,  $\text{Pr}_{2-x}\text{Ce}_x\text{CuO}_{4-\delta}$  and  $\text{La}_{2-x}\text{Sr}_x\text{CuO}_4$ .

The charge-spin separation [14, 15], clearly identifiable Mott-Hubbard (MH), antiferromagnetic and spin crossovers contain generic features which appear to be common for small clusters and large thermodynamic systems [16]. Studies of conventional Mott-Hubbard and magnetic phase transitions [17, 18, 19, 20, 21] have tended to concentrate on macroscopic systems containing a large, and essentially an infinite number of particles. In attempts to address some of the above, the Hubbard model has been discussed within the exact Lieb-Wu (LW) equations in one dimension (1d) [22, 23, 24] and a wide variety of approximation schemes in higher dimensions [25, 26, 27]. Most theories originating from the Bethe-*ansatz*, such as LW, involve coupled nonlinear integral equations that have to be solved numerically

for every set of parameters. Numerical uncertainties associated with such solutions severely limit their applications when calculating subtle features at intermediate values of temperature and other parameters. Although some properties of Hubbard clusters have been calculated [28, 29, 30, 31, 32, 33, 34], many questions remain with regard to microscopic origins of charge-spin separation and pseudogap behavior, short range correlations and weak singularities (*crossovers*) at finite temperature [35, 36].

In this work, we study the phase diagrams for the two and four site Hubbard clusters [16] using analytical diagonalization combined with the grand canonical ensemble in a multidimensional parameter space of temperature  $T$ , magnetic field  $h$ , on-site Coulomb interaction  $U \geq 0$ , and chemical potential  $\mu$  (with hopping parameter  $t = 1$ ). Our calculations for finite clusters are based on the exact analytical expressions for the eigenvalue  $E_n$  of the  $n^{\text{th}}$  many-body eigenstate, grand partition function  $Z$  (where the number of particles  $N$  and the projection of spin  $s^z$  are allowed to fluctuate) and its derivatives without taking the thermodynamic limit and hence involve no approximations. The grand canonical potential  $\Omega_U$  for interacting electrons is

$$\Omega_U = -T \ln \sum_{n \leq N_H} e^{-\frac{E_n - \mu N_n - h s_n^z}{T}}, \quad (1)$$

where  $N_n$  and  $s_n^z$  are the number of particles and the projection of spin in the  $n^{\text{th}}$  state respectively. The dimension  $N_H$  of the Hilbert space in (1) depends on the

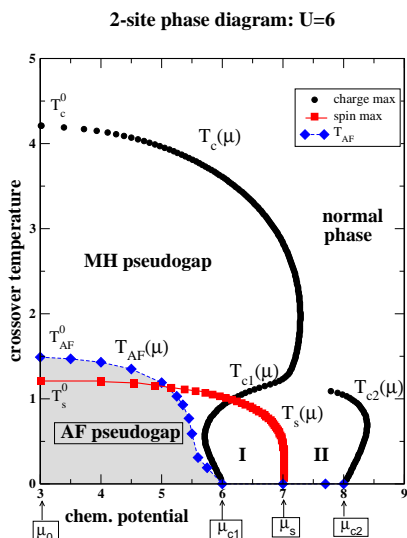


FIG. 1: Temperature  $T$  vs chemical potential  $\mu$  phase diagram for the two site cluster at  $U = 6, h = 0$ . The antiferromagnetic pseudogap phase is shaded and bounded above by  $T_{AF}(\mu)$ . It vanishes in regions I and II, which are charge bifurcation phases representing (pseudo) charge gaps at  $T > 0$ . The charge and spin crossover temperatures  $T_c(\mu)$  and  $T_s(\mu)$  are obtained from maxima in charge and spin susceptibilities. Since there is particle-hole symmetry, only  $\mu$  values above half-filling, i.e.  $\mu > \mu_0$ , are shown. Note that in regions I and II, there is strong charge-spin separation.

number of sites, satisfying  $N_H = 4^2$  for the two site cluster, and  $N_H = 4^4$  for the four site cluster. The electron charge susceptibility  $\chi_c(\mu)$  or the corresponding thermodynamic density of states,  $\rho(\mu) = \frac{\partial \langle N(\mu) \rangle}{\partial \mu}$ , describes the local spectral characteristics of charge excitations and fluctuations in the number of electrons

$$\langle N^2 \rangle - \langle N \rangle^2 = T \frac{\partial \langle N(\mu) \rangle}{\partial \mu}. \quad (2)$$

The spin susceptibility  $\chi_s(\mu)$  or spin density of states  $\sigma(\mu) = \frac{\partial \langle s^z \rangle}{\partial h}$  describes the local spin excitations as parameters  $h, \mu$  or  $T$  are varied, where spin fluctuations  $\langle (\Delta s^z)^2 \rangle$  closely follow the variation of spin susceptibility  $\chi$  with respect to  $\mu$  and  $h$

$$\langle (s^z)^2 \rangle - \langle s^z \rangle^2 = T \frac{\partial \langle s^z \rangle}{\partial h}. \quad (3)$$

Once all the many-body eigenvalues of the Hubbard clusters are known, it is straightforward to calculate the ground state properties and these results are reported elsewhere [16]. Using the same eigenvalues, we have evaluated the exact grand partition function and thermal averages such as magnetization and susceptibilities numerically as a function of the set of parameters  $\{T, h, \mu, U\}$ .

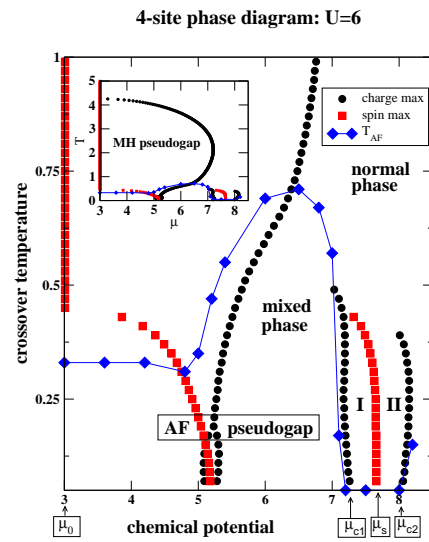


FIG. 2: Temperature  $T$  vs chemical potential  $\mu$  phase diagram for the four site cluster at  $U = 6, h = 0$ . Regions I and II are quite similar to the ones found in the two site cluster, again showing strong charge-spin separation. However, note the (new) mixed phase which consists of charge, spin and AF pseudogaps, that is present in this cluster. The inset shows the same diagram with a larger scale for the crossover temperature. Labels of crossover temperatures are suppressed for clarity.

Using maxima and minima in spin and charge susceptibilities, phase diagrams in a  $T$  vs  $\mu$  plane for any  $U$  and  $h$  can be constructed.

Among many interesting results rich in variety for  $U > 0$ , sharp transitions are found between phases with true charge and spin gaps in the ground state; for infinitesimal  $T > 0$ , these gaps are transformed into ‘pseudogaps’ with some nonzero weight between peaks (or maxima) in susceptibilities monitored as a function of doping (i.e.  $\mu$ ) as well as  $h$ . We have also verified the well known fact that the low temperature behavior in the vicinity of half-filling, with charge and spin pseudogap phases coexisting, represents an antiferromagnetic insulator in the Hubbard clusters [16]. However, away from half filling, we find very intriguing behavior in thermodynamical charge and spin degrees of freedom. At low temperature, new peak structures in the charge  $\chi_c(\mu)$  and zero magnetic field spin  $\chi_s(\mu)$  susceptibilities are observed to develop [16]; between two consecutive peaks, there exists a pseudogap in charge or spin degrees. Opening of such distinct and separated pseudogap regions at low temperature, the signatures of corresponding charge and spin separation, is seen in both the two and four site clusters, away from half filling.

In Fig. 1, we show the phase diagram for the two site cluster at  $U = 6$  and  $h = 0$ , where  $T_c(\mu)$  describes the

high temperature, MH insulator-metal transition as  $\mu$  varies. At low temperature, this dependence bifurcates and  $T_{c1}(\mu)$  and  $T_{c2}(\mu)$  denote the crossover temperatures at lower and higher doping (respectively) corresponding to similar MH like transitions. The low temperature regions I and II, bounded by these crossover temperatures, define a charge bifurcation phase which persists up to a high doping level,  $\mu_{c2}$ . In this charge pseudogap, there are strong spin fluctuations centered around  $\mu_s$  at low temperature which decay when either  $\mu \rightarrow \mu_{c1}$  or  $\mu \rightarrow \mu_{c2}$  (i.e. near the boundaries where charge gaps melt). In the same figure, the antiferromagnetic crossover temperature  $T_{AF}(\mu)$  is obtained by monitoring the spin susceptibility peaks as a function of the applied field at a given chemical potential  $\mu$ , as seen in measurements of Néel temperature doping dependence [12]. If  $h_c$  denotes the field value corresponding to the peak closest to zero,  $T_{AF}$  is defined as the temperature at which the critical field  $h_c(\mu)$  for the onset of magnetization vanishes (melting the AF spin gap).  $T_{AF}$  can also be obtained from zero field staggered spin susceptibility. The spin crossover temperature  $T_s(\mu)$ , associated with the opening of the zero-magnetic-field spin pseudogap in Fig. 1, denotes the temperature below which strong spin pseudogap correlations are observed to develop. This has been suggested as a precursor to superconductivity [37]. Note that spin fluctuations are significantly suppressed below  $T_s$  and how these crossover temperatures and critical  $\mu$  values define various regions such as, a) charge pseudogap, b) AF pseudogap, c) spin pseudogap and d) normal phases.

The four site phase diagram, Fig. 2 with  $U = 6$  and  $h = 0$ , appears to be more complex with several charge bifurcation phases above (or below) half filling, starting at the electron (hole) doping level near 1/8 filling. However, there is a clear self-similarity in the right-most bifurcation region for the 2-site and the 4-site clusters (Figs. 1 and 2). This bifurcation region retains strong charge pseudogap stability as in the two site cluster. We believe that these regions of phase space, with strong spin and charge fluctuations, are quite relevant to the high  $T_c$  cuprates and other similar materials, where doping of electrons or holes introduces dramatic changes in their physical properties.

We have followed the behavior of pseudogaps in this region as a function of the on-site Coulomb repulsion  $U$ . With increasing  $U$ , several features are observed to develop; (a) separation of charge and spin boundaries away from half-filling, (b) opening of a pseudo charge gap, (c) large spin fluctuations inside this charge gap region. This phase with a charge gap closely resembles the inhomogeneous commensurate phase found in Ref.[9], where the mobile holes in the quasi-one dimensional structures (stripes) acquire a spin gap in spatially confined Mott-insulating regions [2, 9].

The doping dependence of the normal-state *spin pseudogap* shows that at low temperature, it is stable in the underdoped regime, persists at optimal doping and dis-

appears in the overdoped regime at  $\mu = \mu_s$ . In the phase diagrams in Figs. 1 and 2 at zero temperature, we notice several quantum phases and corresponding quantum critical points (QCPs), at  $\mu = \mu_{c1}, \mu_s, \mu_{c2}$ . A comparison of the two phase diagrams for the two and four site clusters, in Figs. 1 and 2, reveals many common features in addition to the QCPs. As  $\mu$  increases, there is a sharp transition in both clusters at  $\mu_{c1}$  from a Mott-Hubbard antiferromagnetic insulator into a phase with charge and spin separation and gaps. A similar behavior has been observed experimentally [11, 12] in the cuprates. At critical doping  $\mu_{c1}$ , the antiferromagnetic phase disappears and at higher doping, in regions I and II, the spin and charge pseudogap phases coexist with one another independent of how strong  $U$  is. These two regions are separated by a boundary where the spin gap vanishes. At critical doping  $\mu_s$  with  $T_s \rightarrow 0$ , the zero spin susceptibility  $\chi_s$  at zero temperature exhibits a sharp maximum. Thus the behavior of the critical temperature  $T_s(\mu)$ , which falls abruptly to zero at critical doping  $\mu_s$ , implies [8, 10] that the pseudogap can exist independently of possible superconducting pairing. As mentioned above, as  $T \rightarrow 0$  and  $\mu = \mu_s$ , the spin gap disappears while the charge gap prevails up to  $\mu = \mu_{c2}$ . Upon further doping, the charge gap vanishes at  $\mu_{c2}$  and Fermi liquid behavior is restored due to full charge-spin reconciliation. Figs. 1 and 2 are consistent with the existence of pseudogap phases and quantum phase transitions at  $\mu_s$  in the high  $T_c$  superconductors, when the ground state spin gap disappears [5, 6, 10, 38]. The QCPs separate the spin pseudogap phase from the quantum spin liquid state, coexisting with the charge pseudogap. We have also seen that a reasonably strong magnetic field has a dramatic effect (mainly) on the QCP at  $\mu_s$ .

The spin susceptibility  $\chi_s$  in the underdoped pseudogap region I, defined by  $\mu_{c1} \leq \mu \leq \mu_s$ , displays an anomaly at temperature  $T_s$  below which the spin degrees of freedom become suppressed. The gapped spin excitations imply that spin singlet states which exist between  $T_s$  and  $T_{c1}$  in Fig. 1 can be considered as preformed pairs with properties different from FL. As temperature decreases, approaching  $T_{c1}$  from above,  $\chi_s$  decreases while  $\chi_c$  increases due to strong charge fluctuations in the vicinity of  $T_{c1}$  signaled by a sharp peak in the excitation spectrum, consistent with ARPES measurements [39]. The thermal fluctuations close to the boundaries  $T_{c1}$  of the charge bifurcation phase destroy the charge pseudogap and provide conditions at which the spin pseudogap state coexists with a charge liquid background.

In Figs. 1 and 2, we also show the crossover temperature  $T_{AF}(\mu)$  deduced from maxima in the antiferromagnetic spin fluctuations  $\sigma(\mu)$ . The phase diagram for the two site cluster shows an island of stability for the antiferromagnetic phase and the corresponding crossover temperature,  $T_{AF}(\mu)$ , decreases monotonically as the chemical potential  $\mu$  increases. In the underdoped regime close to half filling, the antiferromagnetic phase in the two site

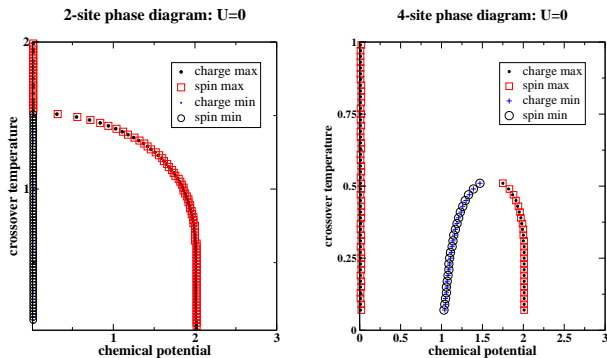


FIG. 3: The single particle or ‘noninteracting’ ( $U = 0$ ) case, illustrating the charge and spin, peaks and valleys for the two and four site clusters. Note how the charge and spin maxima and minima in dos follow one another indicating the absence of charge-spin separation.

cluster is fully separated from the charge bifurcation region. In contrast, the behavior of  $T_{AF}$  with increasing  $\mu$  is nonmonotonic for the four site cluster and there is some overlap (near  $T_{AF} \approx T_{c1}$ ) in the underdoped regime between the antiferromagnetic phase and a charge bifurcation region. At higher doping within the (right-most) bifurcation regime (i.e. regions I and II),  $T_{AF} \equiv 0$  and the charge-spin separation is very similar to that seen in the two site cluster.

As an important footnote, we show how the charge and spin peaks (and valleys) follow one another for both the two and four site clusters when  $U = 0$  in Fig. 3 (in sharp contrast to the  $U = 6$  cases, in regions I and II where charge (as well as spin) maxima and minima are well separated) indicating that there is no charge-spin separation here. In this limiting, single particle case for the two site cluster, there are no temperature driven

charge bifurcation phases away from half filling and hence the corresponding  $T_{c1} \equiv 0$ . In the entire range  $-2t \leq \mu \leq 2t$ , the charge and spin fluctuations directly follow one another, i.e.  $T_{c1} = T_{c2} = T_s$  without charge-spin separation.

In summary, we have illustrated the phase diagram and the presence of temperature driven crossovers, quantum phase transitions and charge-spin separation for any  $U \neq 0$  in the two and four site Hubbard clusters as doping (or chemical potential) is varied. Our bottom-up approach and exact thermodynamics for small clusters, when monitored as a function of doping, displays the presence of clearly identifiable, temperature driven crossovers into new phases and distinct transitions at corresponding QCPs in the ground state, seen in large thermodynamic systems. It appears that the short-range correlations alone are sufficient for pseudogaps to form in small and large clusters, which can be linked to the generic features of phase diagrams in temperature and doping effects seen in the high  $T_c$  cuprates. The pseudogap features and the variations of  $\chi_c$ ,  $\chi_s$ ,  $T_{AF}$  with  $\mu$  as well as the existence of QCPs suggest that the normal state spin singlet pseudogap, closely linked to short range correlations, can also exist in small clusters. The exact cluster solution shows how charge and spin gaps are formed at the microscopic level and their behavior as a function of doping (i.e. chemical potential), magnetic field and temperature. The pseudogap formation can also be associated with the condensation of spin and charge degrees of freedom below (spin and charge) crossover temperatures  $T_s$  and  $T_{c1}$  (respectively). Finally, the two and four sites clusters share very important intrinsic characteristics with the high  $T_c$  superconductors apparently because in all these ‘bad’ metallic high  $T_c$  materials, local interactions play a key role.

This research was supported in part by the U.S. Department of Energy under Contract No. DE-AC02-98CH10886.

- 
- [1] P. W. Anderson, *Science* **235**, 1196 (1987).  
[2] V. Emery and S. A. Kivelson, *Nature (London)*, **374**, 434 (1995).  
[3] T. Timusk and B. Statt, *Rep. Prog. Phys.* **62**, 61 (1999).  
[4] S. A. Kivelson *et al.*, *Rev. Mod. Phys.* **75**, 1201 (2003).  
[5] D. S. Marshall *et al.*, *Phys. Rev. Lett.* **76**, 4841 (1996).  
[6] Andrea Damascelli, Zahid Hussain, Zhi-Xun Shen, *Rev. Mod. Phys.* **75**, 473 (2003).  
[7] P. W. Anderson, *Adv. Rev.* **46**, 3 (1997).  
[8] G. V. M. Williams, J. L. Tallon and J. W. Loram, *Phys. Rev. B* **58**, 15053 (1998).  
[9] V. J. Emery, S. A. Kivelson and O. Zachar, *Phys. Rev. B* **56** 6120 (1997).  
[10] S. D. Obertelli, J. R. Cooper and J. L. Tallon, *Phys. Rev. B* **46**, R14928 (1992).  
[11] Y. Dagan, M. M. Qazilbash, C. P. Hill, V. N. Kulkarni, and R. L. Greene, *Phys. Rev. Lett.* **92**, 167001 (2004).  
[12] P. K. Mang, O. P. Vajk, A. Arvanitaki, J. W. Lynn, and M. Greven, *Phys. Rev. Lett.* **93**, 027002 (2004).  
[13] G. S. Boebinger *et al.*, *Phys. Rev. Lett.* **77**, 5417 (1996).  
[14] V. J. Emery, S. A. Kivelson and H. Q. Lin, *Phys. Rev. Lett.* **64**, 475 (1990).  
[15] A. M. Tsvelik, *Quantum Field Theory in Condensed Matter Physics* (Cambridge University Press) p 275 (1995).  
[16] A. N. Kocharian, G. W. Fernando, K. Palandage and J. W. Davenport, *J. Mag. Mag. Mater.*, in press (2005).  
[17] W. Langer, M. Plischke and D. Mattis, *Phys. Rev. Lett.* **23**, 1448 (1969).  
[18] J. C. Kimball and J. R. Schrieffer, Preprint, University of Pennsylvania (August, 1971).  
[19] J. B. Sokoloff, *Phys. Rev. B* **3**, 3826 (1971).  
[20] L. N. Bulaevski and D. I. Khomskii, *Sov. Phys. Solid State.* **14**, 3015 (1973).

- [21] A. Georges, G. Kotliar, W. Krauth and M. J. Rozenberg, *Rev. Mod. Phys.* **68** 13 (1996).
- [22] E. H. Lieb, and F. Y. Wu, *Phys. Rev. Lett.* **20**, 1445 (1968).
- [23] M. Takahashi, *Thermodynamics of one dimensional solvable models*, Cambridge Univ. Press (1999).
- [24] *The Many-Body Problem: An Encyclopedia of Exactly Solved Models in One Dimension*, ed. by Daniel C. Mattis (World Scientific, 1994).
- [25] C. Huscroft, M. Jarrell, Th. Maier, S. Moukouri and A. N. Tahvildarzadeh, *Phys. Rev. Lett.* **86** 139 (2001).
- [26] S. Moukouri and M. Jarrell, *Phys. Lett.* **16** 167010-1 (2001).
- [27] S. Moukouri *et al.*, *Phys. Rev. B* **61**, 7887 (2000).
- [28] H. Shiba and P. A. Pincus, *Phys. Rev. B* **5**, 1966 (1972).
- [29] J. Callaway, D. P. Chen, and R. Tang, *Phys. Rev.* **B35**, 3705 (1987).
- [30] Claudius Gros, *Phys. Rev. B* **53**, 6865 (1996).
- [31] F. Lopez-Urias and G. M. Pastor, *Phys. Rev. B* **59**, 5223 (1999).
- [32] A. N. Kocharian and Joel H. Sebold, *Phys. Rev. B* **53**, 12804 (1996).
- [33] A. Avella, F. Mancini, and T. Saikawa, *Eur. Phys. J. B* **36**, 445 (2003).
- [34] R. Schumann, *Ann. Phys.* **11**, 49 (2002).
- [35] M. Aizenman and E. H. Lieb, *Phys. Rev. Lett.* **65**, 1470 (1990).
- [36] Y. Nagaoka, *Sol. State Comm.* **3**, 409 (1965); *Phys. Rev.* **147**, 392 (1965).
- [37] Z.-X. Shen *et al.*, *Phys. Rev. Lett.* **70** 1553 (1993); H. Ding *et al.*, *Phys. Rev.* **54**, 1553 (1993).
- [38] C. Castellani, C. Di Castro, and M. Grilli, *Phys. Rev. Lett.* **75**, 4650 (1995).
- [39] H. Ding *et al.*, *Phys. Rev. Lett.* **87**, 227001 (2001).